5. Resistance Characteristics of High Speed Hull Form with Air-ship Form Bulb

by Kazuo Suzuki*, *Member* Mitsuhisa Ikehata*, *Member*
Naoki Mizutani†, *Member* Takeshi Inoue†, *Member*
Hiroshi Hosoi†, *Member*

(*From J.S.N.A. Japan, Vol. 172 Dec. 1992*)

Summary

In the present study, minimization of wave resistance of a special type ship in high speed range is discussed according to the concept of wave making interference between a main hull and an air-ship form bulb. This bulb is formed by the combination of a hydrodynamic point source and a line sink, semi-splitted from the main hull of displacement type and supported by the strut. Wave resistance of this special type ship is minimized under some design conditions by means of nonlinear programming. In this paper, experimental investigations are carried out for two selected models which have the air-ship form bulb and the main hull of the mathematical waterlines and frame lines optimized by the present theory. After showing the model test results of fixed trim conditions and free trim conditions, some discussions about the direction of model improvements are given. In order to adopt the air-ship form bulb as the practical bulbous bow, the effect of an entrance angle of the main hull, the control of the trim and so on are investigated experimentally.

1. Introduction

In recent years, many ideas are proposed in order to pursue the high speed vessel. Many of those ideas are based on unconventional concepts such as the application of hydrodynamic lift generated by wings. In those cases, however, we have many problems for the purpose of sizing up and long distance voyage. As well known, conventional ship, that is a displacement type, has more merits than unconventional ones at least from point of view of buoyancy. Therefore it can be considered as one of the effective ways to pursue the high speed vessel based on the concept of displacement type.

Many ships operating on seaway now have conventional bulbous bows, which can reduce the wave resistance by the hydrodynamic interaction of the waves between the main hull and the bulb. However, results of the minimum wave resistance theory [1] show that, the higher speed the optimum bulb radius becomes the larger. In a practical sense, those results are not applicable to most high speed ships of displacement type.

In the case of the bulb expressed by a point doublet, the optimum position calculated by means of the nonlinear programming changes widely in respective design Froude number [2]. In high speed range, the wave length of elementary waves generated by a disturbance becomes so large that the so-called wave making length becomes large too. According to this consideration, the relative position of the bulb to the main hull is one of the important design factors.

In the present study, the air-ship form bulb is introduced instead of the conventional bulb. This bulb is formed by the combination of a hydrodynamic point source and a line sink, semi-splitted from the main hull and supported by the strut as shown in Fig. 1 or 2 in the next section. In the case of the air-ship form bulb, the optimum bulb radius can be suppressed smaller than the conventional one in high speed range. The degree of freedom of hull form design is increased by the employment of this air-ship form bulb concept, because we can select the bulb position arbitrarily under required design constraints. The position of the bulb should be fixed at the fore end of

*Faculty of Engineering, Yokohama National University
†Graduate School, Yokohama National University

the main hull as far as we adopt the conventional concept.

Series calculations about the minimum wave resistance hull forms with the air-ship form bulb by means of the nonlinear programming are shown in the reference [3]. In this paper, more detailed experimental investigations are carried out for two hull form models selected from results of those series calculations.

2. Hull Form with Air-ship Form Bulb

As illustrated in Fig. 1 or 2, the composite hull form which consists of the main hull, the air-ship form bulb and its strut, is employed in this paper. In order to optimize the hull form, namely, minimize the wave resistance, each hull form component must be expressed by mathematical formulae. As illustrated in Fig. 1 and 2, the right hand Cartesian coordinate system fixed on the advancing ship with the origin at the midship on the still water plane and x-axis forward is used, in which coordinates x, y, z are normalized by the half ship length $\ell = L/2$ and fluid velocities are normalized by the advancing velocity of the ship U. For the sake of convenience, the main hull is presented as the following elementary ship.

$$y = f(x)g(z) \tag{1}$$

The shape of the waterline $f(x)$ and the shape of the frame line $g(z)$ are defined respectively as follows,

$$f(x) = \pm \sum_{n=1}^{N} \left\{ a_n \cos\left[(n - \frac{1}{2})\pi \frac{x - x_0}{1 + x_0} \right] + b_n \sin\left[n\pi \frac{x - x_0}{1 + x_0} \right] \right\}, \tag{2}$$

$$g(z) = 1 - \left| \frac{z}{t} \right|^{\beta}, \tag{3}$$

where x_0 is x-coordinate of the midship of the main hull, and t is the normalized draft as follows when the real draft is given by T.

$$t = T/\ell \tag{4}$$

As in eq. (3), the shape of the frame line is approximated by the parabola of the order β.

The air-ship form bulb is expressed as the axisymmetric streamline body formed by the point source with the normalized strength m and the uniform line sink with the total strength $-m$ and the normalized length $2a$ [4]. The position of the point source, namely, the fore end of the line sink is $(x_A,\ 0,\ -t_A)$ and the aft end of the line sink is $(x_B,\ 0,\ -t_A)$. The length of the air-ship form bulb is defined as the length of the line sink. The following relations exist,

$$a = (L_A/2)/\ell = L_A/L, \tag{5}$$

$$t_A = T_A/\ell, \tag{6}$$

where L_A is the length of the air-ship form bulb as defined above and T_A is the real depth of the bulb center. This bulb must be supported by the strut having the waterline shape of the second order parabola such as

$$y = \pm \frac{b_S}{c^2} \left(c^2 - \{x - (1 - c)\}^2 \right), \tag{7}$$

where

$$b_S = (B_S/2)/\ell = B_S/L, \tag{8}$$

$$c = (L_S/2)/\ell = L_S/L. \tag{9}$$

L_S and B_S express the length and the breadth of the strut respectively.

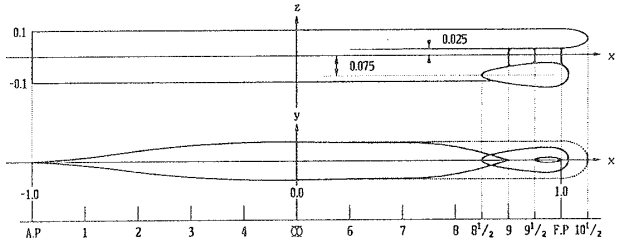

Fig. 1 Outline profile of model AS-1.

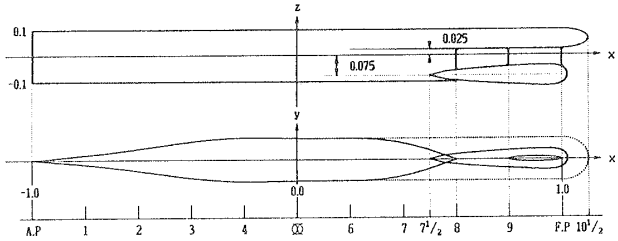

Fig. 2 Outline profile of model AS-2.

In order to formulate the minimum wave resistance problem based on the concept of the air-ship form bulb, an objective function and design constraints have to be defined. As the objective function, the following wave resistance coefficient based on the linear wave resistance theory is employed,

$$C_w = R_w/(1/2)\rho U^2 L^2 = 8\pi\gamma_0^2 \int_0^{\pi/2} (\{P(\theta)\}^2 + \{Q(\theta)\}^2) \sec^3\theta d\theta, \tag{10}$$

where

$$\gamma_0 = g\ell/U^2. \tag{11}$$

Amplitude functions $P(\theta)$ and $Q(\theta)$ can be expressed by the principle of linear superposition as follows.

$$\left.\begin{matrix} P(\theta) \\ Q(\theta) \end{matrix}\right\} = \left\{\begin{matrix} P_M(\theta) \\ Q_M(\theta) \end{matrix}\right\} + \left\{\begin{matrix} P_S(\theta) \\ Q_S(\theta) \end{matrix}\right\} + \left\{\begin{matrix} P_A(\theta) \\ Q_A(\theta) \end{matrix}\right\} \tag{12}$$

The first and second term of the right hand side of the above equation represent wave making effects of the main hull and the strut respectively. In both cases, Michell's thin ship theory is used. The third term represents a wave making effect of the air-ship form bulb, which is composed of amplitude functions for the point source and the line sink [5]. The detailed formulae for numerical calculation of these amplitude functions are given in Appendix.

The objective function (10) should be minimized under suitable design constraints. At first, the following equality constraint is introduced to keep the displacement constant.

$$\frac{8t}{\pi}\frac{\beta}{\beta+1}\sum_{n=1}^{N}\frac{a_n\lambda}{2n-1}\sin\frac{(2n-1)\pi}{2} + \frac{8}{3}t_S b_S c + 4\pi m a = 8\frac{\nabla}{L^3} \tag{13}$$

This constraint is described as the linear form with respect to design variables explained below. In the third term of eq. (13), that means the displacement of the air-ship form bulb, the approximate formula is used to linearize the equation with respect to m. In eq. (13),

$$\lambda = (L_M/2)/\ell = L_M/L, \tag{14}$$

where L_M is the length of the main hull, and

$$t_S = T_S/\ell. \tag{15}$$

In addition, the following inequality constraints are imposed.

$$f(x_0 + ih) < f(x_0 + (i-1)h) \tag{16}$$

$$f(x_0 - ih) < f(x_0 - (i-1)h) \tag{17}$$

In this paper, $i = 1, \ldots, 10$ and $h = \lambda/10$ are selected. Eqs. (16), (17) express that the waterline breadth of the main hull decreases toward the bow and the stern respectively from its midship.

In ordinary cases, coefficients $a_1 \sim a_N, b_1 \sim b_N$ of eq. (2) expressing the waterline shape of the main hull and the strength m of the point source expressing the bulb size can be selected as design variables. In this paper, for the series coefficients, $N = 3$ is selected. Futhermore, as a special case of the present problem, the position of the point source, namely, x_A can be selected as a design variable in order to optimize the position of the air-ship form bulb [3]. These design variables are determined through the optimization process to minimize the objective function (10) under the prescribed design constraints eqs. (13), (16) and (17) by means of nonlinear programming. Many nonlinear optimization techniques are developed up to the present. From those techniques, a combined method of SUMT (Sequential Unconstrained Minimization Technique) [6] and GPM (Gradient Projection Method) [7] is employed, in which linear equality constraints can be satisfied by GPM and inequality constraints can be satisfied by SUMT respectively [8].

3. Investigations Based on Model Tests

3.1 Experiments of Original Models

Concerning the series calculations shown in the reference [3], two examples are selected for the purpose of the experimentally comparative investigation of resistance characteristics of the optimum hull form with the air-ship form bulb.

Table 1 Particulars of original models.

Particulars of Models			
Model		AS-1	AS-2
Design Froude Number	F_n	0.500	
Length	L	1.500 m	
Breadth	B	0.108 m	0.126 m
Draft	T	0.075 m	
Length of Main Hull	L_M	1.350 m	1.200 m
Length of Air-ship Form Bulb	L_A	0.225 m	0.375 m
Length of Strut	L_S	0.075 m	0.150 m
Breadth of Strut	B_S	0.015 m	
Order of Parabolic Frame Line	β	4	
Displacement Volume	∇	0.00665 m^3	0.00666 m^3
Wetted Surface Area	S	0.2933 m^2	0.2872 m^2
Displacement Length Ratio	∇/L^3	0.00197	0.00197
Block Coefficient	C_b	0.5473	0.4698
Prismatic Coefficient	C_p	0.6841	0.5873
Midship Area Coefficient	C_m	0.8000	

Particulars of two selected original models are given in Table 1. The main hull of model AS-1 and AS-2 has 90 % and 80 % length of the total one respectively. In both cases, the design Froude

number is 0.5, the order of parabolic frame line is 4, and the displacement length ratio is selected as 0.002, which is about the lower limit of the actual value of high speed ships of displacement type in the past. In Table 1, however, the displacement length ratios are slightly different from the designed one, because eq. (13) that is the displacement constraint is the approximate formula as explained previously. Outline profiles of both models are illustrated in Fig. 1, 2, and body plans are shown in Fig. 3, 4. As compared with model AS-1, model AS-2 has larger breadth, smaller block coefficient and smaller wetted surface area.

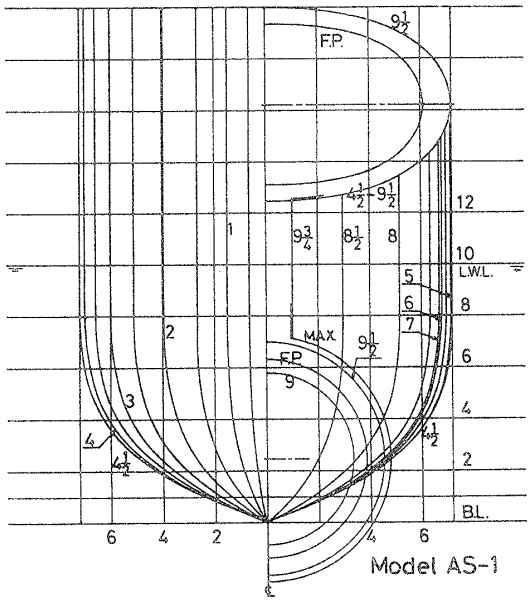

Fig. 3 Body plan of model AS-1.

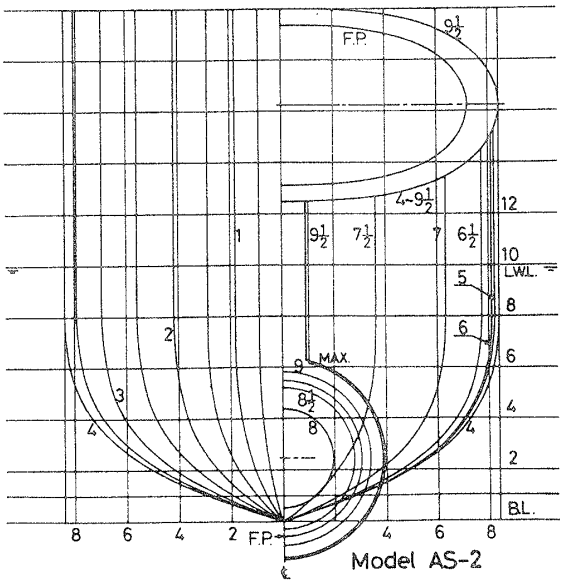

Fig. 4 Body plan of model AS-2.

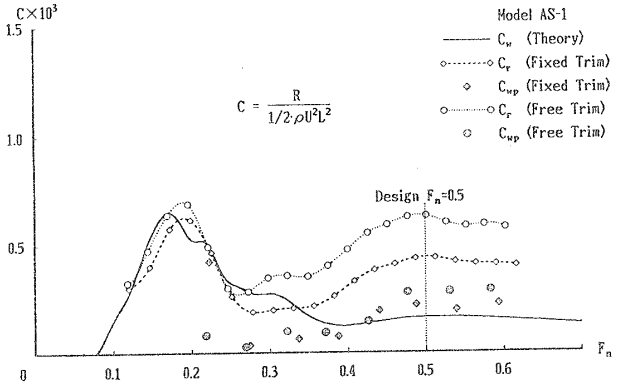

Fig. 5 Experimental results of model AS-1.

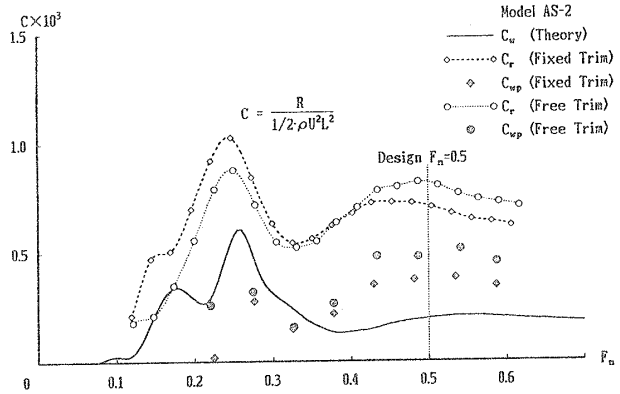

Fig. 6 Experimental results of model AS-2.

Model tests are carried out for fixed trim conditions and free trim conditions. Test results of models AS-1 and AS-2 are given in Fig. 5 and 6 respectively. In these figures, residuary resistance coefficients C_r obtained from the towing test using Schoenherr's friction coefficients and wave pattern resistance coefficients C_{wp} based on the wave analysis are shown together with theoretical wave resistance coefficients C_w. Differences between the experimental results C_r, C_{wp} and the theoretical results C_w become large in high F_n range, and differences between fixed and free trim conditions are also observed. Since the optimum hull forms in this paper are obtained from the application of the linear wave resistance theory, in which the effect of change of trim is not taken into account, theoretical estimations for free trim conditions would be supposed worse. Comparing two results for fixed trim conditions, however, theoretical wave making effects of the hydrodynamical singularities expressing the main hull and the air-ship bulb are not true, especially in high F_n range. It can be also considered that other resistance components are related

with those differences, because these hull forms are more complex than the conventional ones. In order to search those reasons and realize the resistance reduction, the separation flow at the aft part of the bulb, the effect of the entrance angle of the main hull, the control of trim and so on are investigated experimentally in the following sections.

3.2 Modifications of Models

According to the above discussions, effects of

1. the aft part shape of the bulb
2. the bulb shape under the keel line
3. the entrance angle of the main hull
4. the trim control

are investigated experimentally by modifications of original models AS-1 and AS-2. As for the 1st item, the aft part of the bulb connected with the main hull is faired to eliminate the effect of separation flow on this part. As for the 2nd item, the bulb shape under the keel line in Fig. 3 or 4 is cut and faired from the practical point of view. As for the 3rd item, the entrance angle of the main hull is decreased, because relation between the entrance angle and the spray resistance is reported for a displacement type high speed ship [9]. Finally, as for the 4th item, the effect of trim control by horizontal small fins attached at the stern of both sides is studied, because the change of trim by the large air-ship form bulb becomes remarkable in high F_n range. In the present study, original models AS-1 and AS-2 are modified and tested according to the above procedure. Therefore the latter models keep the effects of former modifications.

Table 2 Kinds of modified models.

Kinds of Models			T.T.		W.A.	
model name		experimental condition	fix	free	fix	free
AS-1	-2	original	○	○	○	○
AS-1FR	-2FR	fairing of aft part of bulb	○	○	-	-
AS-1W	-2W	cut of bulb under keel line	○	○	-	-
AS-1EA	-2EA	decrease of entrance angle	○	○	-	○
AS-1FIN	-2FIN	with stern horizontal fin	-	○	-	○
T.T. : Towing Test, W.A. : Wave Analysis fix, free : trim condition						

In Table 2, model names are assigned respectively and experimental plans are summarized. Sectional area curves of models AS-1, AS-1FR and AS-1W are compared in Fig. 7, and those of models AS-2, AS-2FR and AS-2W are compared in Fig. 8. Water line curves of models AS-1 and AS-1EA are compared in Fig. 9, and those of models AS-2 and AS-2EA are also compared in same figure. The entrance angle of both models AS-1EA and AS-2EA is 10 deg. in each side.

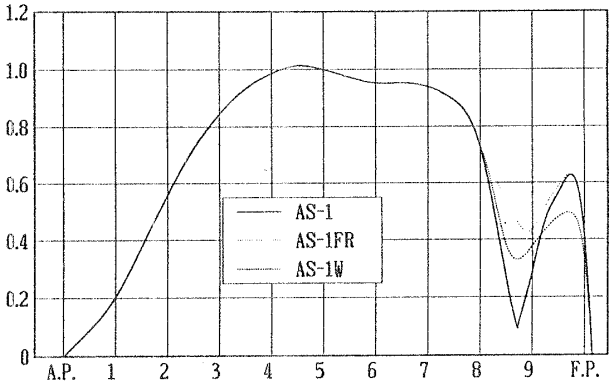

Fig. 7 Comparison of sectional area curve.

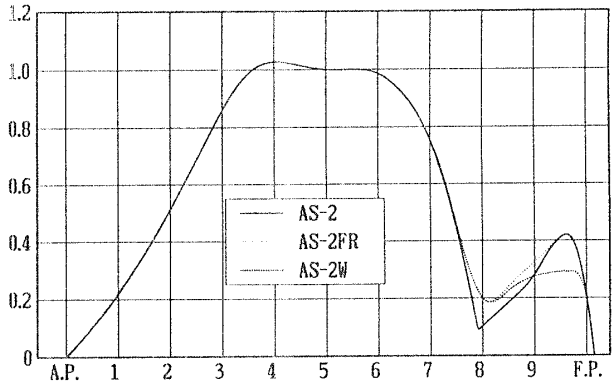

Fig. 8 Comparison of sectional area curve.

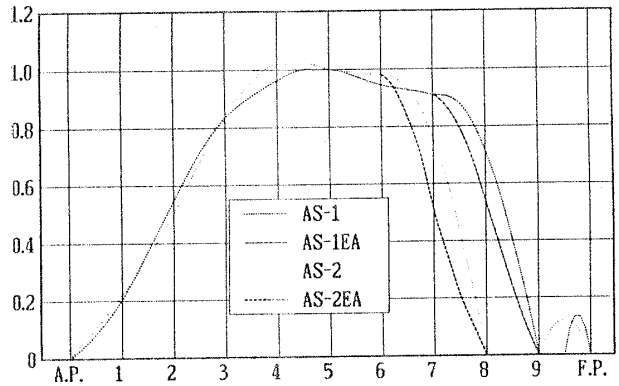

Fig. 9 Comparison of waterline curve.

In Fig. 10, configurations of stern attached with horizontal fins of models AS-1FIN and AS-2FIN are illustrated. Increments of the wetted

surface area by stern horizontal fins are 1.20 % and 1.15 % for models AS-1FIN and AS-2FIN respectively. The size of fin is determined from the estimated moment to need to restore the change of trim at design F_n of original models shown in the subsequent figures (Fig. 19 and Fig. 21).

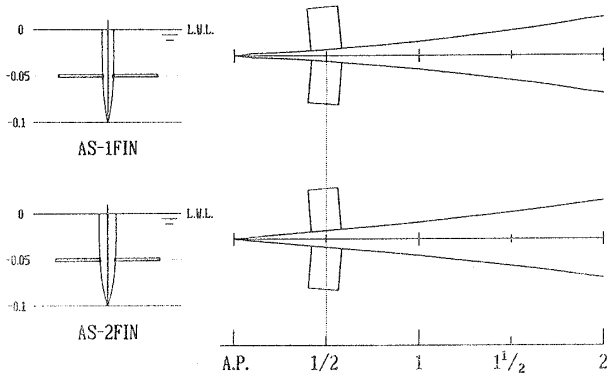

Fig. 10 Position of stern horizontal fin.

3.3 Experiments of Modified Models

According to the experimental plans explained in the previous section, test results of modified models are shown and discussed. At first, experimental results of AS-1, AS-1FR, AS-1W and AS-1EA in fixed trim conditions are shown in Fig. 11, and those in free trim conditions are shown in Fig. 12. In the same way, experimental results of model AS-2 series are shown in Fig. 13 and 14.

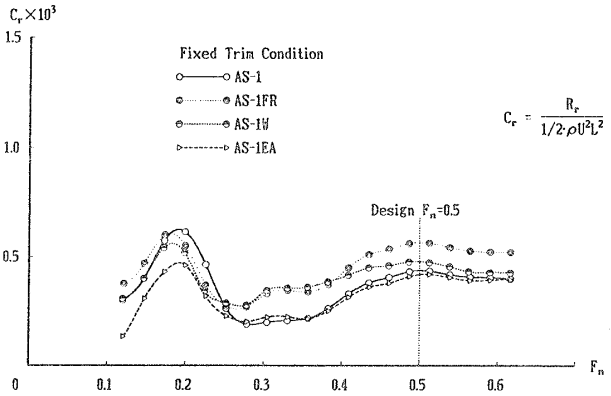

Fig. 11 Experimental results of AS-1 series in fixed trim condition.

Since it can be assumed that pure effects of respective modifications appear in experiments of fixed trim conditions, test results shown in Fig. 11 and 13 are discussed. The resistance reduction at design F_n is observed in cases of hull forms FR and W of model AS-2 series. In those of model AS-1 series, however, the resistance reduction can not be seen. In both series, the hull form EA with the small entrance angle shows the resistance reduction, especially model AS-2EA shows fairly large resistance reduction.

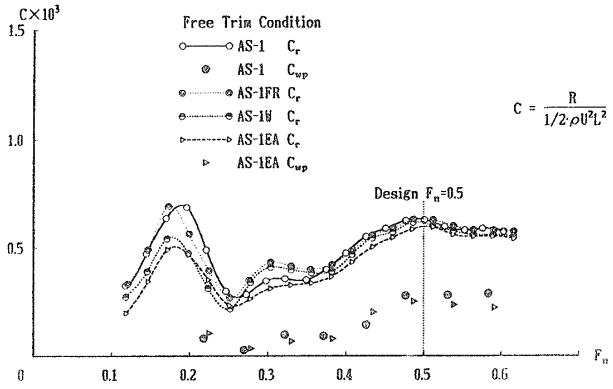

Fig. 12 Experimental results of AS-1 series in free trim condition.

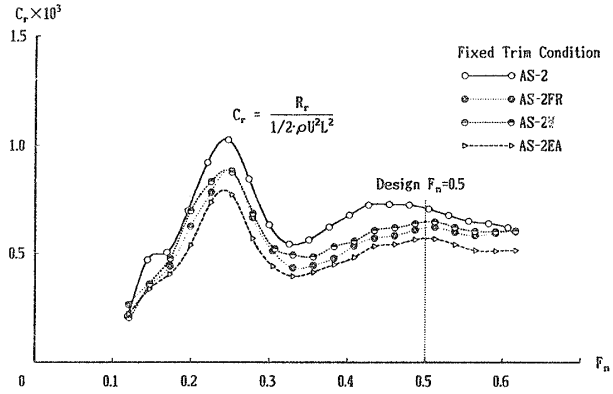

Fig. 13 Experimental results of AS-2 series in fixed trim condition.

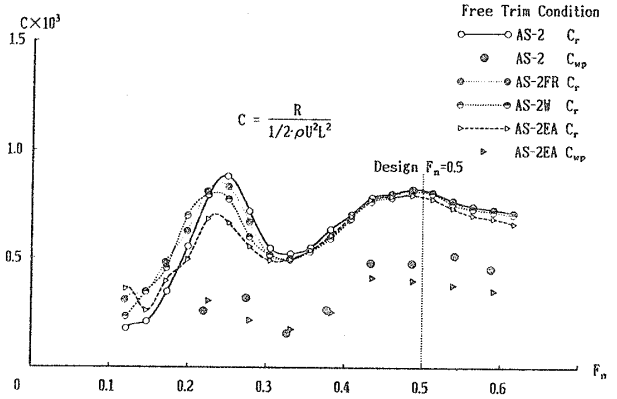

Fig. 14 Experimental results of AS-2 series in free trim condition.

In experiments of free trim conditions, which are important in practice, the above mentioned effects disappear as shown in Fig. 12 and 14,

that is, all types of hull form in both AS-1 and AS-2 series have almost same resistance characteristics at design F_n. The effects of the small entrance angle become smaller than those in fixed trim conditions.

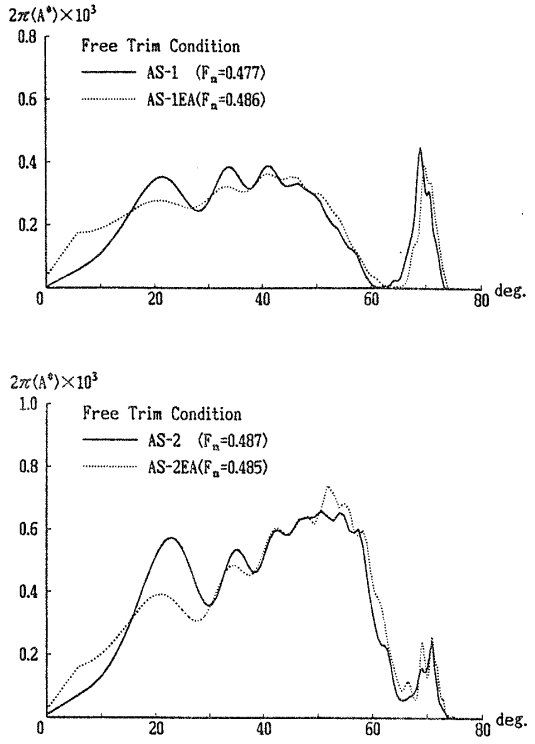

Fig. 15 Comparison of wave spectrum.

For models AS-1EA and AS-2EA in free trim conditions, wave analyses are carried out to investigate wave making characteristics about hull forms with the small entrance angle. Their wave pattern resistance coefficients obtained by wave analyses are compared with those of models AS-1 and AS-2 in Fig. 12 and 14 respectively. Wave spectra at design F_n are also compared in Fig. 15 with respect to these hull forms. As well known, the relation between the wave pattern resistance coefficient and the wave spectrum in Fig. 15 is as follows,

$$C_{wp} = 2\pi \int_0^{\pi/2} \{A^*(\theta)\}^2 d\theta, \qquad (18)$$

where $A^*(\theta)$ is a non-dimensionalized weighed amplitude function, having the follwing relation with the amplitude functions $P(\theta)$, $Q(\theta)$ as,

$$\{A^*(\theta)\}^2 = 4\gamma_0^2(\{P(\theta)\}^2 + \{Q(\theta)\}^2)\sec^3\theta. \quad (19)$$

As shown in Fig. 15, characteristics of free waves in free trim conditions are almost same for original models and EA models of respective series. If the resistance characteristics are different with respect to original models and EA models, it can be expected that flow phenomena around the bow near field, for example phenemena of spray, are different.

As discussed above, the significant resistance reduction can not be obtained by modified hull forms FR, W and EA of both series, in free trim conditions. As final modified models, AS-1FIN and AS-2FIN to suppress the change of trim by stern horizontal fins are tested. Experimental results of these models in free trim conditions are shown in Fig. 16 and 17 including the results of original models. In both FIN models, residuary resistance and wave pattern resistance are reduced at design F_n as in these figures. In particular, the resistance reduction of model AS-2FIN is observed in whole F_n range as shown in Fig. 17.

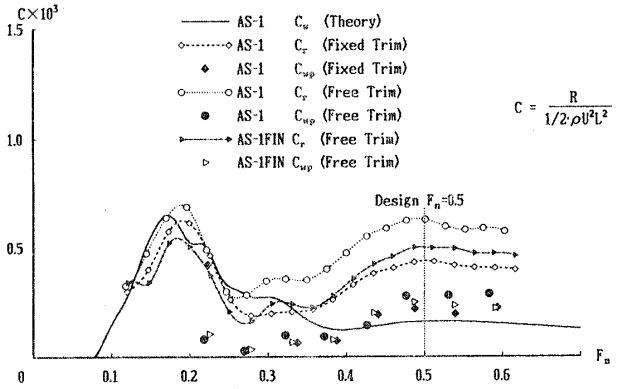

Fig. 16 Experimental results of model AS-1 and AS-1FIN.

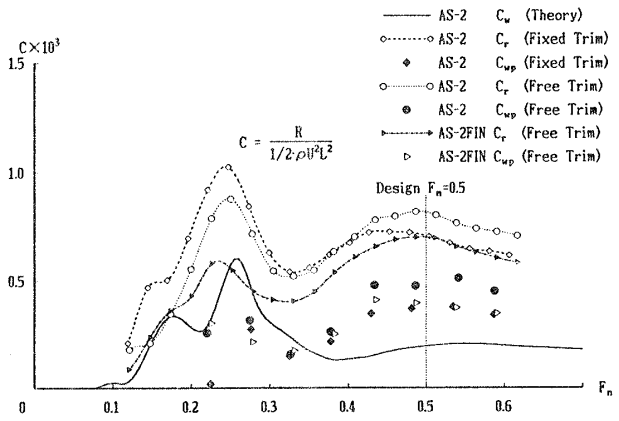

Fig. 17 Experimental results of model AS-2 and AS-2FIN.

Wave making characteristics of FIN models are shown in Fig. 18 as the comparison of wave spectra at design F_n, in which spectra of the original

models in both trim conditions are also given. As shown in this figure, wave making characteristics of FIN models in free trim conditions are similar to those of original models in fixed trim conditions, because of suppression of the change of trim.

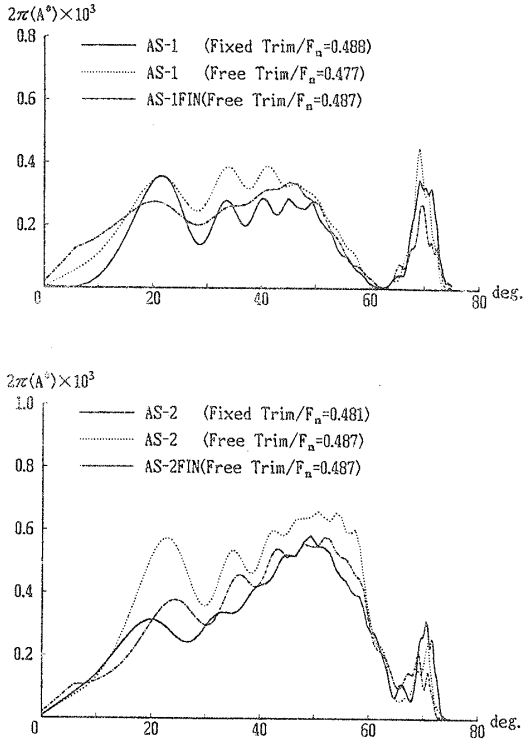

Fig. 18 Comparison of wave spectrum.

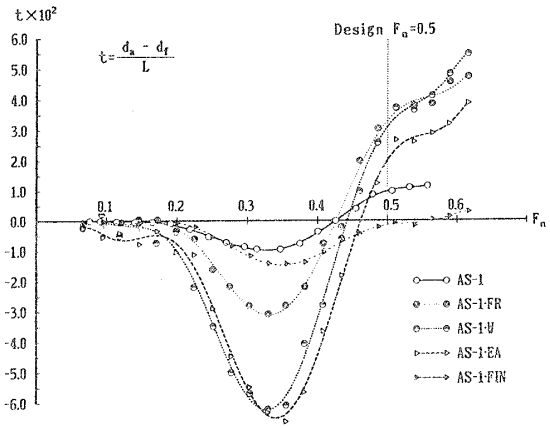

Fig. 19 Comparison of trim of AS-1 series.

Additionally, changes of trim and sinkage are also measured as shown in Fig. 19, 20 for all models of AS-1 series, and in Fig. 21, 22 for all models of AS-2 series. In high F_n range, large trim caused by the lift of the air-ship form bulb is observed with respect to FR, W and EA models, and for same models large sinkage is also measured. In the case of FIN models, however, the trim is restored to horizontal level and the sinkage is reduced at the same level of original models by the effect of stern horizontal fins, which are related to the resistance reduction. As discussed here, changes of trim and sinkage are particularly important in high F_n range.

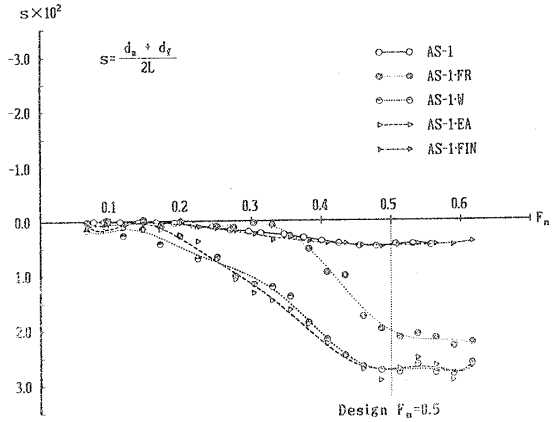

Fig. 20 Comparison of sinkage of AS-1 series.

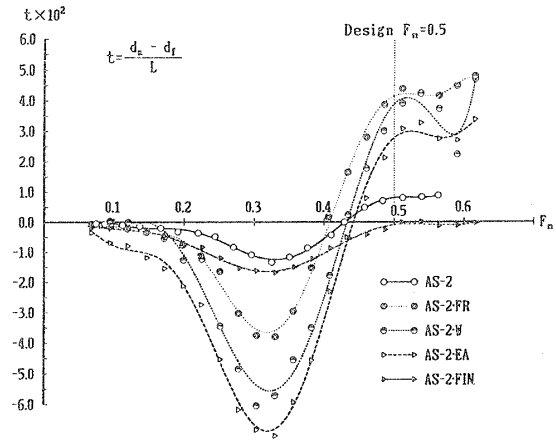

Fig. 21 Comparison of trim of AS-2 series.

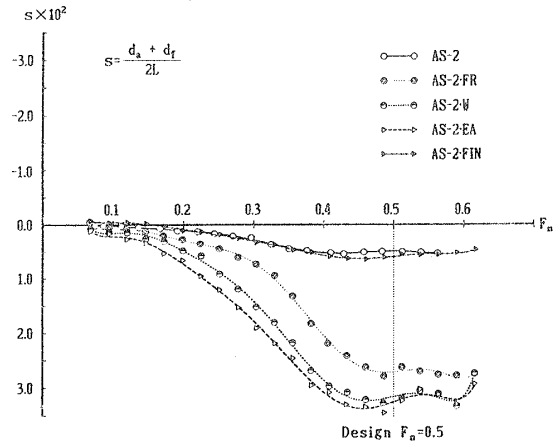

Fig. 22 Comparison of sinkage of AS-2 series.

As the last figure, the effective drag lift ratios appered in ref. 10) are estimated as 200 m length ships with the air-ship form bulb by using the

present experimental results about model AS-1 and AS-1FIN. These are shown in Fig. 23, where HP is the hourse power of respective transport vehicles. In these estimations, the pay load W_p is assumed as 30% of the total displacement and the propulsive coefficient is assumed as 0.6. As shown in Fig. 23, it can be expected that the ships with the air-ship form bulb are more efficient than conventional hydrofoiles.

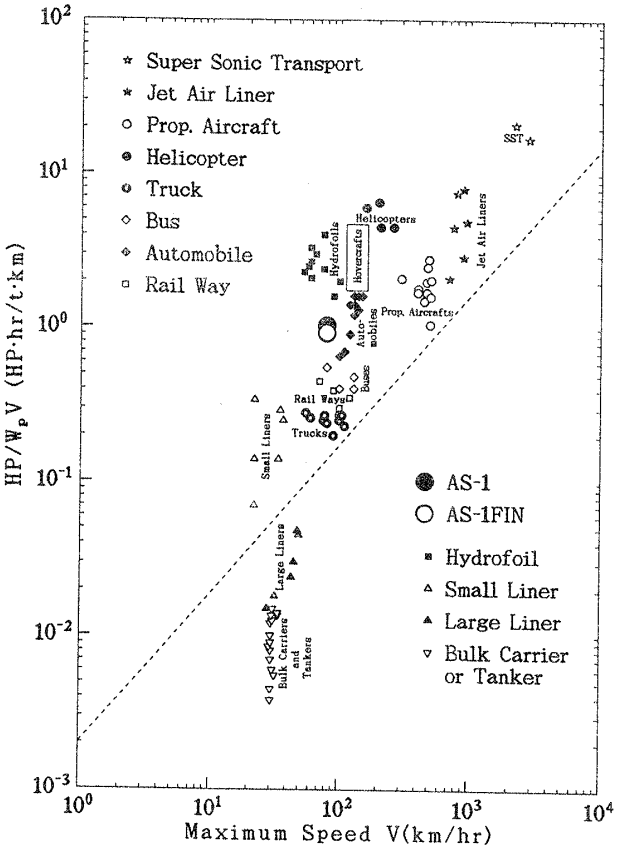

Fig. 23 Effective drag lift ratio.

4. Conclusions

In the present paper, the air-ship form bulb which reduces the wave resistance in high speed range by the hydrodynamical interaction with the main hull has been proposed. The composite hull form with the air-ship form bulb and its strut has been optimized to minimize the wave resistance based on the linear theory under suitable design constraints by means of nonlinear programming. For two selected models, detailed experimental investigations have been carried out. The main conclusions of this paper are as follows.

1. In experimental results of the original models with the air-ship form bulb, differences between the experimental results and the theoretical results are seen to become large in high F_n range, and differences between fixed and free trim conditions are also observed.

2. Concerning to these results, effects of the aft part shape of the bulb (FR model), the bulb shape under the keel line (W model), the entrance angle of the main hull (EA model) and the trim control by stern horizontal fins (FIN model) have been investigated experimentally. However, the significant resistance reduction can not be obtained by FR, W and EA models modified from the original models, in free trim conditions.

3. In the case of FIN models to suppress the change of trim by stern horizontal fins, at the design F_n, the trim is restored to horizontal level, and resistance characteristics are improved. The change of trim and sinkage are particularly important in high F_n range.

4. By estimation of the effective drag lift ratio from the experimental results, it can be expected that the ships with the air-ship form bulb are more efficient than conventional hydrofoiles.

The authors wish to express their deep appreciations to Mr. H. Yamasaki and Mr. I. Okada of Yokohama National University for their kind cooperations in model testing. This study is partially supported by the Grant-in Aid for Scientific Research of the Ministry of Education, Science and Culture of Japan (No. 04650397).

References

1) Maruo, H., Kasahara, K. and Miyazawa, M. : Ship Forms of Minimum Wave Resistance with Bulbs, Journal of Soc. of Naval Arch. of Japan, Vol. 135 (1974).

2) Suzuki, K. and Maruo, H. : Fundamental Studies on Hull Form Design by Means of Nonlinear Programming (4th Report) - Minimum Wave Resistance Problem with Special Reference to the End Shape Effect -, Journal of Soc. of Naval Arch. of Japan, Vol. 153 (1983) (in Japanese).

3) Suzuki, K. and Ikehata, M. : Minimization of Wave Resistance Based on the Concept of Air-ship Form Bulb, HULL FORM '92, Inchon, Korea (1992).

4) Milne-Thomson, L. M. : *Theoretical Hydrodynamics*, 5th edition, Macmillan (1968), p.482.

5) Jinnaka, T., Tsutsumi, T. and Ogiwara, S. : Hull Form Design Derived from Wave Analysis, Int. Seminar on Wave Resistance, Tokyo (1976).

6) Rosen, J. B. : The Gradient Projection Method for Nonlinear Programming, Part I - Linear Constraints-, SIAM Journal Appl. Math., Vol. 8, No. 1 (1960).

7) Kowalik, J. and Osborn, M. R. : *Method for Constrained Optimization Problems*, Elsevier (1968).

8) Asano, K., Kondo, K., Toyofuji, M. and Sugita, S. : Vibration Analysis of Rectangular Stiffened Plate Immersed in Water by Means of Direct Energy Minimization, Journal of the Kansai Soc. of Naval Arch., Japan, Vol. 175 (1979) (in Japanese).

9) Takarada, N., Ikehata, M., Suzuki, K., Takai, M., Sasaki, N. and Shigematsu, K. : R & D of a Displacement-Type High Speed Ship (Part 2. Resistance and Propulsion), FAST'93, Yokohama (1993).

10) Akagi, S. : *Transport Vehicle Engineering*, Corona, (1971) (in Japanese).

Appendix

1. Amplitude functions of main hull,

$$\left.\begin{matrix} P_M(\theta) \\ Q_M(\theta) \end{matrix}\right\} = -\frac{1}{2\pi}\int_{-t}^{0}\left\{1-\left|\frac{z}{t}\right|^{\beta}\right\}e^{\gamma_0 z\sec^2\theta}dz \times \sum_{n=1}^{N}\left\{\begin{matrix} I_n(\theta) \\ J_n(\theta)\end{matrix}\right\}$$

where,

$$\left.\begin{matrix} I_n(\theta) \\ J_n(\theta) \end{matrix}\right\} =$$

$$a_n M_n\left[\mp\frac{1}{M_+(\theta)}\begin{matrix}\sin\\ \cos\end{matrix}(\mu_+(\theta))\sin(\mu_+^*(\theta)) - \frac{1}{M_-(\theta)}\begin{matrix}\sin\\ \cos\end{matrix}(\mu_-(\theta))\sin(\mu_-^*(\theta))\right]$$

$$+b_n N_n\left[\frac{1}{N_+(\theta)}\begin{matrix}\cos\\ \sin\end{matrix}(\nu_+(\theta))\sin(\nu_+^*(\theta)) \pm \frac{1}{N_-(\theta)}\begin{matrix}\cos\\ \sin\end{matrix}(\nu_-(\theta))\sin(\nu_-^*(\theta))\right]$$

and

$$M_\pm(\theta) = M_n \pm \gamma_0\sec\theta,$$
$$N_\pm(\theta) = N_n \pm \gamma_0\sec\theta,$$
$$\mu_\pm(\theta) = (2M_n \pm \gamma_0\sec\theta)x_0,$$
$$\nu_\pm(\theta) = (2N_n \pm \gamma_0\sec\theta)x_0,$$
$$\mu_\pm^*(\theta) = (M_n \pm \gamma_0\sec\theta)(1+x_0),$$
$$\nu_\pm^*(\theta) = (N_n \pm \gamma_0\sec\theta)(1+x_0),$$
$$M_n = \frac{(n-1/2)\pi}{1+x_0}, \quad N_n = \frac{n\pi}{1+x_0}.$$

2. Amplitude functions of strut,

$$\left.\begin{matrix} P_S(\theta) \\ Q_S(\theta) \end{matrix}\right\} = \frac{2b_S}{\pi c^2}\frac{1-e^{-\gamma_0 t_S\sec^2\theta}}{\gamma_0^3\sec^4\theta} \times \left\{\begin{matrix} \sin(\gamma_0(1-c)\sec\theta) \\ \cos(\gamma_0(1-c)\sec\theta)\end{matrix}\right.$$
$$\left.\begin{matrix} \times\{\gamma_0 c\sec\theta\cos(\gamma_0 c\sec\theta) - \sin(\gamma_0 c\sec\theta)\} \\ \times\{-\gamma_0 c\sec\theta\cos(\gamma_0 c\sec\theta) + \sin(\gamma_0 c\sec\theta)\}\end{matrix}\right\}.$$

3. Amplitude functions of air-ship form bulb,

$$\left.\begin{matrix} P_A(\theta) \\ Q_A(\theta) \end{matrix}\right\} = \frac{me^{-\gamma_0 t_A\sec^2\theta}}{\gamma_0(x_A-x_B)\sec\theta} \times \left\{\begin{matrix} \gamma_0(x_A-x_B)\sec\theta\cos(\gamma_0 x_A\sec\theta) \\ \gamma_0(x_A-x_B)\sec\theta\sin(\gamma_0 x_A\sec\theta)\end{matrix}\right.$$
$$\left.\begin{matrix} -\sin(\gamma_0 x_A\sec\theta) + \sin(\gamma_0 x_B\sec\theta) \\ +\cos(\gamma_0 x_A\sec\theta) - \cos(\gamma_0 x_B\sec\theta)\end{matrix}\right\}$$

where $(x_A, 0, -t_A)$ is the position of point source, namely, the fore end of line sink, and $(x_B, 0, -t_A)$ is the aft end of line sink.